MOLECULAR AND CELLULAR BIOLOGY, June 1995, p. 3291–3300 Vol. 15, No. 6
0270-7306/95/$04.00+0

Analysis of the *Saccharomyces cerevisiae* Mitochondrial *COX3* mRNA 5′ Untranslated Leader: Translational Activation and mRNA Processing

GERLINDE WIESENBERGER, MARIA C. COSTANZO, AND THOMAS D. FOX*

Section of Genetics and Development, Cornell University, Ithaca, New York 14853-2703

Received 11 November 1994/Returned for modification 24 January 1995/Accepted 23 March 1995

We used transformation of yeast mitochondria and homologous gene replacement to study features of the 613-base *COX3* mRNA 5′ untranslated leader (5′-UTL) required for translational activation by the protein products of the nuclear genes *PET54*, *PET122*, and *PET494* in vivo. Elimination of the single AUG triplet in the 5′-UTL had no detectable effect on expression, indicating that activator proteins do not work by allowing ribosomes to bypass that AUG. Deletion of the entire 5′-UTL completely prevented translation, suggesting that the activator proteins do not function by antagonizing any other negative element in the 5′-UTL. Removal of the 15 terminal bases from the 5′ end of the 5′-UTL did not block activator-dependent translation. The largest internal deletion that did not interfere with translation removed 125 bases from the upstream portion of the leader. However, two large deletions that blocked translation could be reverted to activator-dependent expression by secondary changes in the remaining 5′-UTL sequences, indicating that the original deletions had not removed the translational activator target but only deformed it. Taken together, the deletion mutations and revertants define a region of 151 bases (between positions −480 and −330 relative to the start codon) containing sequences that are sufficient for translational activation when modified slightly. Suppression of the respiratory phenotypes of two 5′-UTL mutations by overexpression of *PET54*, *PET122*, and *PET494* indicated functional interactions between the leader and the three activator proteins. The mature *COX3* mRNA is cleaved from a precursor immediately downstream of the preceding $tRNA^{Val}$ in a fashion resembling mRNA processing in vertebrate mitochondria. Our results indicate that the site of this cleavage in *Saccharomyces cerevisiae* is determined solely by the position of the tRNA.

Translation of the mitochondrially coded *COX3* mRNA depends specifically on the products of three nuclear genes, *PET54*, *PET122*, and *PET494* (reviewed in references 10, 24, and 45). The protein products of these genes are located in mitochondria, associated with the inner membrane (33), and they physically interact with each other (4). They activate translation through a site located in the 613-base *COX3* mRNA 5′ untranslated leader (5′-UTL) (9). Translation of at least two other mitochondrial mRNAs, *COX2* (39) and *COB* (46), is also activated specifically through their 5′-UTLs, and evidence suggesting a similar mechanism for translation of several other mRNAs in this system has been reported (reviewed in reference 43).

The *COX3* mRNA-specific translational activator proteins appear to function by mediating the interaction of mitochondrial ribosomes with the mRNA 5′-UTL. This conclusion is based on studies of genetic interactions among components of this system: the PET122 protein functionally interacts with small-subunit mitochondrial ribosomal proteins (20–22, 34), while both PET54 and PET122 functionally interact with the mRNA 5′-UTL (4, 11). Thus, these studies suggest a model in which the translational activator complex tethers the mRNA to the membrane by binding to a site in the 5′-UTL and activates localized synthesis of the highly hydrophobic cytochrome oxidase subunit III by promoting the binding of ribosomes to the mRNA.

Seven of the eight major yeast mitochondrial mRNAs have long 5′-UTLs, ranging in approximate size from 300 to 950 bases, and the generation of at least five of these mRNAs involves cleavage of a precursor molecule to generate the 5′ end (reviewed in reference 14). All seven of the long 5′-UTLs contain at least one AUG triplet upstream of the translation initiation codon (19). The presence of these upstream AUG triplets suggests that mitochondrial ribosomes do not scan for initiation codons like cytoplasmic ribosomes (28, 49), but there is no experimental evidence bearing on this question. Site-directed mutagenesis has established the importance of AUG in the recognition of initiation sites and also indicated that other sequences or structures play a role in defining such sites (15, 40). However, a Shine-Dalgarno pairing mechanism (50) does not appear to be involved (10, 43). In many ways, translation initiation in yeast mitochondria appears to resemble the internal ribosomal entry process that occurs on some viral and cellular mRNAs in animal cell cytoplasms (26, 30, 44, 54).

Mitochondrial transformation and gene replacement by homologous recombination (15) have made possible in vivo deletion analysis of functional sites encoded in mitochondrial DNA (mtDNA) (11, 36, 37). In this study, we used this strategy to test the function of mutated *COX3* mRNAs in vivo to better define the RNA sequences necessary for translational activation. Our results suggest that activation in this system does not involve antagonism of intrinsically negative elements in the 5′-UTL and demonstrate that a limited portion of the 613-base 5′-UTL can function as a target for translational activators. In addition, analysis of the mRNAs produced by several of our mutants strongly indicates that 5′ processing of the *COX3* mRNA is directed by the $tRNA^{Val}$ immediately upstream in the precursor transcript and thus resembles mRNA processing events in vertebrate mitochondria (38, 42).

* Corresponding author. Mailing address: Section of Genetics and Development, Cornell University, Biotechnology Building, Ithaca, NY 14853-2703. Phone: (607) 254-4835. Fax: (607) 255-6249. Electronic mail address: tdf1@cornell.edu.

TABLE 1. Yeast strains used in this study

Strain	Nuclear [mitochondrial] genotype	Source or reference
DL2	*MAT***a** *lys2* [*rho*$^+$]	15
GW14	*MAT***a** *lys2* [*rho*$^+$ *cox3-160*]	This study
GW15	*MAT***a** *lys2* [*rho*$^+$ *cox3-429*]	This study
GW16	*MAT***a** *lys2* [*rho*$^+$ *cox3-438*]	This study
GW17	*MAT***a** *lys2* [*rho*$^+$ *cox3-446*]	This study
GW22	*MAT***a** *lys2* [*rho*$^+$ *cox3-421*]	This study
GW50	*MAT***a** *lys2* [*rho*$^+$ *cox3-512*]	This study
GW51	*MAT***a** *lys2* [*rho*$^+$ *cox3-516*]	This study
GW52	*MAT***a** *lys2* [*rho*$^+$ *cox3-481*]	This study
GW53	*MAT***a** *lys2* [*rho*$^+$ *cox3-476*]	This study
GW84	*MAT***a** *ade2 leu2-3,112 ura3-52* [*rho*$^+$ *cox3-438*]	This study
GW93	*MAT***a** *lys2* [*rho*$^+$ *cox3-67*]	This study
GW94	*MAT***a** *lys2* [*rho*$^+$ *cox3-60*]	This study
GW111	*MAT***a** *lys2* [*rho*$^+$ *cox3-4*]	This study
GW139	*MAT***a** *lys2* [*rho*$^+$ *cox3-662*]	This study
GW140	*MAT***a** *lys2* [*rho*$^+$ *cox3-666*]	This study
GW141	*MAT***a** *lys2* [*rho*$^+$ *cox3-652*]	This study
GW146	*MAT***a** *ade2 leu2-3,112 ura3-52* [*rho*$^+$ *cox3-662*]	This study
MCC90rho^0	*MAT*α *pet54-5 ura3-52* [*rho*^{0}]	13
MCC103rho^0	*MAT*α *pet494-41 ura3-52* [*rho*^{0}]	This study
MCC109rho^0	*MAT*α *ade2-101 ura3-52 kar1-1* [*rho*^{0}]	11
MCC118	*MAT***a** *lys2* [*rho*$^+$ *cox3-5*]	15
MCC125	*MAT***a** *lys2* [*rho*$^+$ *cox3-10*]	11
MCC125/DA1	*MAT***a**/*MAT*α *lys2*/*LYS2 ade2*/*ADE2* [*rho*$^+$ *cox3-10*]	This study
MCC126	*MAT***a** *lys2* [*rho*$^+$ *cox3-18*]	This study
MCC129	*MAT***a** *lys2* [*rho*$^+$ *cox3-11*]	11
MCC162	*MAT***a** *lys2* [*rho*$^+$ *cox3-12*]	This study
PTY22	*MAT***a** *ade2 leu2-3,112 ura3-52* [*rho*$^+$]	P. E. Thorsness
TWM21-11Brho^0	*MAT*α *pet122-6 ura3-del ade2* [*rho*^{0}]	T. W. McMullin

MATERIALS AND METHODS

Strains and media. The *Saccharomyces cerevisiae* strains used in this study are listed in Table 1. All strains are isogenic to D273-10B, except MCC109. *rho*^{0} derivatives of yeast strains were obtained by growing cultures for about 30 generations in YPD medium (defined below) containing 50 μg of ethidium bromide per ml. *Escherichia coli* DH5α was used for propagation of plasmids.

Yeast strains were grown in complete medium YP (1% yeast extract, 2% Bacto Peptone) containing the following carbon source(s): 2% glucose (YPD), 2% galactose (YPGal), 2% raffinose (YPR), or 3% ethanol and 3% glycerol (YPEG). Synthetic minimal medium (0.67% yeast nitrogen base) containing 2% glucose (SD) or 2% galactose (SGal) was supplemented as previously described (48) when appropriate. *E. coli* strains were cultured in LB or TB (31).

Transformation of *E. coli*, yeast nuclei, and yeast mitochondria. *E. coli* cells were transformed by the $CaCl_2$ procedure (31). For yeast nuclear transformation, cells were treated with lithium acetate and polyethylene glycol (25). Yeast mitochondrial transformation was performed by high-velocity microprojectile bombardment as described previously (11, 16), except that the helium-driven PDS 1000 (Bio-Rad) was used. The wild-type *COX3* mRNA 5′-UTL-coding region was replaced in mtDNA by mutant alleles as follows. Plasmids bearing the mutations were introduced into the mitochondria of strain MCC109rho^0, and the resulting transformants were mated to strain MCC118, carrying a wild-type mitochondrial genome except for *cox3-5*, a deletion of the entire leader and part of the structural gene (11). Cytoductants in which the large deletion *cox3-5* had been replaced by the desired mutant alleles were identified by crosses to tester strains in a genetic scheme that has been described previously (11).

In vitro construction of *COX3* mRNA 5′-UTL mutations. Plasmids containing mutations in the *COX3* mRNA leader (see Table 2) were derived from plasmids pMC241 (11), pLSF600 (15), pMC240, pGW107, and pGW114. The sequence of this region is available under GenBank accession number J01478; the 5′ end of the 5′-UTL, at position −613 relative to the AUG initiation codon, corresponds to position 189 of this GenBank sequence. pMC240 contains mtDNA from the *Hae*III site upstream of the *COX3* promoter to the *Xba*I site at the 5′ end of the *COX3* 5′-UTL in the plasmid pBluescript(−). pGW107 and pGW114 were derived from pLSF600 and pMC241, respectively, by destroying the *Xba*I site downstream of *COX3*; thus, these plasmids contain only a single *Xba*I site whose position corresponds roughly to the 5′ end of the *COX3* mRNA.

Construction of deletion mutations *cox3-10* and *cox3-11* was described previously (11). A point mutation named *cox3-18* (G-to-A change at position −470) was constructed within the *COX3* 5′-UTL-coding region by oligonucleotide-directed in vitro mutagenesis (29) of pMC241 by using the reagents and strains provided in the Muta-Gene Phagemid kit (Bio-Rad) and the oligonucleotide 5′-TAAATTATTGATAATATCTTC. Following mitochondrial transformation and insertion of *cox3-18* into otherwise wild-type mtDNA, the DNA sequence of the *rho*$^+$ mtDNA was determined from positions −440 to −611 to verify the gene replacement (16). Plasmid pMC257 was created by the same method by using the oligonucleotide 5′-CATTGATAAGATCTTC to create a *Bgl*II site by changing the A at −479 to a C. The deletion *cox3-12* (removing nucleotides −593 to −1) was similarly generated by using the oligonucleotide 5′-CTTTCTAAAT GTGTCATTATAATATTATATCTAGA.

For construction of pGW160, two partially overlapping oligonucleotides (5′-AATCTAGATATAATATTATATCTATC and 5′-GATGTCTACTTCTTTCT AAATGTGTCATAAGATAGATATAATAT) were hybridized, filled in with Sequenase (3), cut with *Acc*I and *Xba*I, and ligated into pGW114 that had been cleaved with the same enzymes, replacing a 631-bp fragment containing part of the wild-type leader and seven codons of the open reading frame with a 46-bp fragment containing a deleted leader and the wild-type coding sequence. For construction of pGW429, pGW446, pGW438, and pGW421, plasmid pGW107 was cut with *Sac*I and *Xba*I, digested with exonuclease III and nuclease S1, treated with Klenow, and religated in the presence of an *Xba*I linker (TCTAGA). Clones were screened for the presence of a single *Xba*I site, and deletions of appropriate sizes and candidates were sequenced. Four clones with deletions of 6, 15, 200, and 412 bp at the 5′ end of the *COX3* leader were digested with *Xba*I and *Xho*I, and the inserts were ligated into pMC240 that had been cut with *Xba*I and *Xho*I, creating pGW429, pGW446, pGW438, and pGW421. For construction of pGW512, pLSF600 was cut with *Pac*I, treated with T4 DNA polymerase, and subsequently cut with *Cla*I. The 1.8-kb fragment containing part of the *COX3* 5′-UTL, the coding sequence, and the 3′ trailer was cloned into pMC240 which had been digested with *Xba*I, treated with Klenow polymerase, and cut with *Cla*I. The deletion was verified by DNA sequence analysis. pGW516 was derived from pMC257, which was linearized with *Bgl*II, treated with Klenow, and cut with *Cla*I. The resulting 1.8-kb fragment, containing part of the *COX3* 5′-UTL, the coding sequence, and the 3′ trailer, was ligated into pMC240, which had been treated as described above for construction of pGW512. DNA sequence analysis revealed that this clone had a deletion of one G from the expected sequence so that both the *Xba*I and *Bgl*II sites were reconstructed. Therefore, *cox3-516* has a deletion of 125 bp and a single-base-pair substitution (A to C) at position −479 with respect to the wild-type *COX3* sequence. Plasmids pGW476 and pGW481 were derived from pGW429 and pGW446, respectively, by *Xba*I digestion, treatment with mung bean nuclease, and religation. Plasmids lacking the *Xba*I site were sequenced.

Plasmids pGW652, pGW662, and pGW666 were obtained by PCR from pMC241Δ1 (11), pMC255 (carrying *cox3-13*; see below), or pMC250 (carrying *cox3-15* [11]), respectively, by using the primer pair 5′-GCTCTAGATATTAT CAATGATTTATA (positions −480 to −462) and 5′-GGTCATGGTGAAGG CATAAC, which is complementary to the mRNA (+49 to +68). Upon digestion with restriction enzymes *Xba*I and *Acc*I, the PCR products were cloned into pGW114 cut with the same enzymes, creating pGW652, pGW662, and pGW666, respectively.

For construction of pGW560 and pGW567, two pairs of oligonucleotides (5′-CTAGATATTCAATACAAATATGACACATTTAGAAAGAAGT plus 5′-CTACTTCTTTCTAAATGTGTCATATTTGTATTGAATAT and 5′-CTAG ATAT T TAAATAAATTATATTCAATACAAATATGACACAT T TAGAAA GAAGT plus 5′-CTACTTCTTTCTAAATGTGTCATATTTGTATTGAATA TAATTTATTTAAATAT) were hybridized and subsequently ligated to the backbone of *Xba*I-*Acc*I-cut pGW114 as described for construction of pGW160. pGW221 was constructed by cloning a 1.9-kb *Xba*I-*Eco*RI fragment containing sequences from downstream of *COX3* into *Xba*I- and *Eco*RI-digested pMC240, creating a complete deletion of *COX3* (*cox3-4*). All of the constructs described above were sequenced (47) prior to transformation to confirm the correct sequences. Mutations *cox3-10*, *cox3-18*, *cox3-160*, *cox3-446*, *cox3-429*, and *cox3-421* were also sequenced after integration into mtDNA.

Selection and analysis of respiration-competent revertants of *COX3* 5′-UTL deletion mutations. Single-colony clones of diploid strain MCC125/DA1 (Table 1) bearing the *cox3-10* deletion (see Fig. 1) (11) were grown in YPD medium and spread on YPEG plates. Spontaneous revertants were streaked on YPEG plates to check for mitotic instability of respiratory growth, a hallmark of heteroplasmic mitochondrial gene rearrangements that bypass the *COX3* translational activation system (8, 41). Of 55 *cox3-10* revertants isolated, 44 exhibited mitotic instability while 11 did not. Sporulation of these 11 mitotically stable diploids revealed that all contained mitochondrial suppressors of *cox3-10*; they exhibited 4:0 segregation of respiratory competence. The locations of two suppressors, *cox3-13* and *cox3-14*, in mtDNA were determined by *rho*$^-$ mapping (16). Haploids carrying the revertant genomes were treated with ethidium bromide to induce *rho*$^-$ deletions, which were then mated to a *cox3-10* mutant strain to identify those that retained the suppressor mutation. The suppressor-carrying *rho*$^-$ derivatives were next mated to tester strains to determine which mitochondrial genetic markers were linked to the suppressor mutation. Both of the suppressors tested were completely linked to *cox3* but not to *cox2*. mtDNA was prepared from each of five such strains and from the wild type as previously described (16). The 1.6-kb *Xba*I fragment carrying the *COX3* 5′-UTL-coding region, the structural gene, and the 3′ trailer was isolated from each strain and cloned into pBluescript(−) (Stratagene). The nucleotide sequence of the entire 5′-UTL-coding region from each clone was determined by the dideoxy-chain termination method (47).

Revertants of strain GW16 carrying the *cox3-438* mutation (see Fig. 1 and Table 2) were similarly isolated on YPEG. Spontaneous revertant colonies of different sizes were streaked on YPEG plates and then tested for mitotic stability. All of the *cox3-438* revertants analyzed were mitotically stable. When crossed to a *rho*^{0} strain with an isogenic nuclear background, all revertants produced respiring diploids, ruling out recessive nuclear suppressors. The revertants were treated with ethidium bromide to remove their mtDNA. The resulting *rho*^{0} strains were then crossed to an isogenic strain carrying the *cox3-438* mutation. Production of respiring diploids from this cross indicated a dominant nuclear suppressor. Failure to yield respiring diploids indicated that the *cox3-438* suppressor was a mitochondrial mutation. The results of these analyses were further confirmed by cytoduction experiments (7). Linkage of nuclear suppressors to *PET54*, *PET122*, or *PET494* was determined by crossing the revertant strains to *rho*^{0} strains carrying the respective *pet* mutations (MCC90rho^0, TWM21-11Brho^0, and MCC103rho^0; see Table 1) and then performing tetrad analysis. To identify the mitochondrial suppressors of *cox3-438*, cellular DNA was isolated (48) and the *COX3* leader region was amplified by the PCR using the primers 5′-GTTTTACACACGAAAGATTATAGG and 5′-GGTCATGGTGAAGGCA TAAC. The PCR products were directly sequenced by the dideoxy-chain termination method (47). To confirm that the single-base-pair changes identified in the *COX3* 5′-UTL were responsible for suppression, the PCR products were cloned, sequenced, and then reintroduced into otherwise wild-type mitochondria by mitochondrial transformation as described above.

RNA gel blot hybridization analysis. Yeast strains were grown in YPGal medium to an optical density at 600 nm of approximately 1.5, and total nucleic acids were prepared as previously described (51). Single-stranded RNAs were subsequently precipitated in 1.6 M LiCl at −20°C and washed with 80% ethanol. A 6-μg sample of total RNA was denatured in a buffer containing 6.5% formaldehyde and 50% formamide and loaded on a 1% agarose gel containing 5.9% formaldehyde in 10 mM sodium phosphate buffer (pH 7), electrophoresed, and blotted onto nitrocellulose. The filter was hybridized with a radioactively labeled probe generated by random priming (Boehringer Mannheim) on the 1.2-kb *Acc*I-*Xba*I fragment containing the *COX3* coding sequence and 3′-flanking sequences. For normalization, the filters were rehybridized with a radiolabeled probe specific for the actin mRNA (17). *COX3* and *ACT1* mRNA levels were quantitated with a Betascope 603 blot analyzer (Betagen Corp.).

Primer extension analysis of mRNA 5′ ends. Mitochondrial RNA was extracted from purified mitochondria (56) by following the protocol for total RNA isolation described above, except that no glass beads were used. Oligonucleotides oxi2c (5′-ATTTATTAATATTAAAAGGA; −406 to −388) and oxi2b (5′-TA AATTTATATATAATTCAA; −214 to −195) were labeled with ^{32}P by using T4 polynucleotide kinase (3) and hybridized to 20 μg of mitochondrial RNA in 50 mM Tris-HCl (pH 8.2)–50 mM KCl by heating the reaction mixture to 65°C for 3 min, chilling it in dry ice-ethanol, and subsequently thawing it on ice. The primer extension reaction was carried out in the presence of 50 mM Tris-HCl (pH 8.2)–5 mM $MgCl_2$–5 mM dithiothreitol–0.5 mM GTP–0.5 mM CTP–1 mM ATP–1 mM TTP–8 U of avian myeloblastosis virus reverse transcriptase (Life Sciences) at 37°C for 20 min. Size markers were generated with sequencing reactions by using the same oligonucleotide primers and the corresponding plasmid DNA templates. The reactions were analyzed on a 6% sequencing gel (3).

Plasmids directing overproduction of translational activator proteins. All of the plasmids used to overproduce the three translational activator genes carried the *ADC1* promoter and terminator derived from plasmid pAAH5 (2). For overexpression of *PET494*, plasmid pMC210 (11) was used. *PET54* overexpression was directed by pTM110A (33) or pGW614 bearing the *ADE2* marker, which was constructed by replacing a 2.2-kb *Bgl*II fragment in pTM110A with a 3.6-kb *Bam*HI fragment from pL909 (18) carrying *ADE2*. *PET122* overexpression was directed by pAD122-74 (33) or pEAD122 (33). Empty vectors pAAH5, YEp352 (23), and pGW608 were used for controls. pGW608 was constructed by disrupting the *LEU2* gene in pAAH5 with *ADE2* as described for pGW614.

RESULTS

Mutation of the single AUG triplet within the *COX3* 5′-UTL has no effect on translation. In the cytoplasmic translation systems of eukaryotes, AUG codons in 5′-UTLs usually inhibit translation since ribosomes typically scan from the 5′ ends of mRNAs and initiate translation at the first AUG encountered (28, 49). AUG codons within the 5′-UTLs of mitochondrial mRNAs are a common feature in *S. cerevisiae* (10, 19). The *COX3* mRNA contains one, at position −472 relative to the start of translation. If mitochondrial ribosomes utilized a scanning mechanism, then the single upstream AUG codon in the *COX3* mRNA might inhibit translation. In this case, the *COX3*-specific translational activators could be involved in overcoming this inhibition.

To test this hypothesis, we changed the G residue of this codon to A in vitro and integrated the mutated gene into the mitochondrial genome in place of the wild-type *COX3* gene as described in Materials and Methods, creating the *cox3-18* allele. The resulting AUA codon should have greatly interfered with any translation initiation at this site (15, 40). Furthermore, since the wild-type *COX3* 5′-UTL contains 98 AUA triplets, this additional AUA should be inconspicuous. Elimination of the AUG codon had no detectable effect on respiratory growth of mutant strain MCC126 (as measured by colony size on YPEG medium) at 13.5, 16, 24, 30, or 37°C. Furthermore, strains carrying *cox3-18* still required translational activators *PET54*, *PET122*, and *PET494*, as shown by crosses of MCC126 to *rho*^{0} null mutant strains affected in each of these three nuclear genes (MCC90rho^0, TWM21-11Brho^0, and MCC 103rho^0 [Table 1]) and subsequent tetrad analyses. Thus, the mechanism of translational activation on the *COX3* mRNA does not require a G residue at position −470 and therefore probably does not involve recognition of the upstream AUG codon by scanning ribosomes. Consistent with this interpretation, revertants of a deletion mutation (*cox3-438*) that exhibit activator-dependent translation (described below) also lack this upstream AUG and flanking sequences.

Large deletions, producing *COX3* mRNAs with extremely short 5′-UTLs, block translation. Another possible mechanism for activation of *COX3* mRNA translation by *PET54*, *PET122*, and *PET494* is that the activators overcome an intrinsically negative feature of the *COX3* 5′-UTL, such as an unfavorable secondary structure. Such mechanisms have been demonstrated in cases of positive translational control in bacteria (1, 55). If this were the case, then removing the long 5′ leader

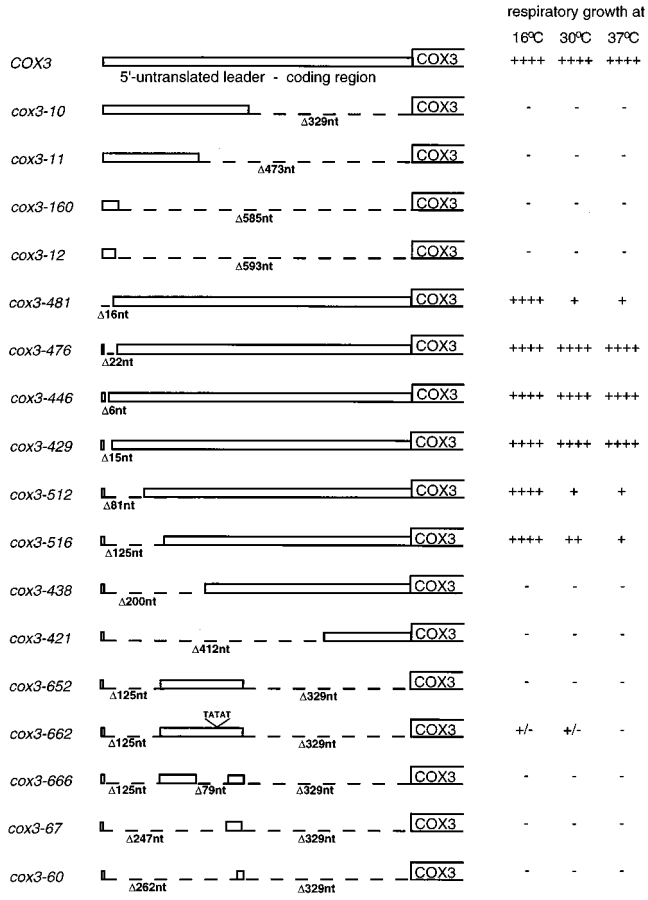

FIG. 1. Structures and respiratory phenotypes of *COX3* 5′-UTL mutations. The 5′-UTL sequences present in wild-type (*COX3*) and mutant mRNAs are indicated by the thin, open boxes. Deleted 5′-UTL sequences (Materials and Methods) are indicated by dashed lines. The thick open boxes indicate the start of the *COX3* structural gene. Respiratory growth was judged by relative colony size on solid media containing ethanol and glycerol as nonfermentable carbon sources. Cells were streaked on YPEG medium incubated for 6 days at 30 or 37°C and for 15 days at 16°C. The precise deletion endpoints, confirmed by DNA sequence analysis, are given in Table 2. nt, nucleotides; −, no growth; +/−, weak growth; +, ++, +++, and ++++ indicate relative colony sizes.

from the *COX3* mRNA might eliminate the need for the activators.

We introduced two large deletions into the 5′-UTL coding region of *COX3*: *cox3-12* deleted bases −593 to −1, while *cox3-160* deleted bases −585 to −1 (Fig. 1 and Table 2). Strains bearing either of these mutations, MCC162 and GW14 (Table 1), failed to grow on nonfermentable carbon sources (YPEG; Fig. 1). RNA gel blot hybridization revealed that the *cox3-160* mutant mRNA accumulated to approximately 50% of the wild-type level (Fig. 2) while the *cox3-12* mRNA accumulated to approximately 13% of the wild-type level (data not shown). Both the *cox3-160* (Fig. 3) and *cox3-12* (data not shown) mutants failed to synthesize detectable coxIII protein. As shown below, other *cox3* mutations caused accumulation of even lower levels of *COX3* mRNA, yet they were able to grow on YPEG and produce the coxIII protein (Fig. 1, 2, and 3). Thus, we concluded that the respiratory growth defects of the *cox3-160* and *cox3-12* deletion mutants result from an inability to translate the mutant mRNAs.

We attempted to recover mitotically stable respiring revertants of the *cox3-12* and *cox3-160* mutants without success. (A single revertant of MCC162 was isolated, but it was mitotically unstable, indicating that a 5′-UTL from another mitochondrial mRNA had been fused to the *COX3* coding region by an mtDNA rearrangement [8, 41].) These results suggest that removal of the *COX3* mRNA 5′-UTL removes the target of a factor required positively to activate translation. However, it remains possible that the leader could contain an undetected negative control site as well.

The 5′-terminal sequences of the mature *COX3* mRNA are not required for translational activation or for mRNA processing. Previous work had demonstrated that sequences in the upstream half of the *COX3* mRNA 5′-UTL are required for translational activation (9, 11). To test the possibility that these sequences are very close to, or at, the 5′ end of the mRNA, we generated short deletion mutations in this region.

The *cox3-476* mutation deleted the 22 bases from −608 to −587, leaving the 5′ end at −613 (see below) intact (Fig. 1 and Table 2). The strain carrying this mutation, GW53, was indistinguishable from the wild type with respect to respiratory growth and its pattern of mitochondrial translation products (Fig. 1 and 3). Two other short deletions in this region, *cox3-446* and *cox3-429*, behaved similarly (Fig. 1 and Table 2). Translation of the *cox3-476* and *cox3-429* mRNAs was shown to be dependent on *PET54*, *PET122*, and *PET494* by crosses to *rho*^{0} strains carrying the respective nuclear mutations (MCC90rho^0, TWM21-11Brho^0, and MCC103rho^0; Table 1) and tetrad analyses.

A fourth short deletion, *cox3-481*, removed the 16 bases at the 5′ end of the message (−613 to −598; Fig. 1 and Table 2). The strain carrying this mutation, GW52, exhibited reduced growth on YPEG relative to the wild type at 30 and 37°C but not at 16°C (Fig. 1). Synthesis of the coxIII protein was reduced at 30°C but easily detectable (Fig. 3). The amount of the mutant mature transcript was reduced to approximately 31% of the wild-type amount at 30°C (Fig. 2) and also at 16°C (data not shown), but both the wild type and the *cox3-481* mutant accumulated slightly larger amounts of *COX3* mRNA at the lower temperature (data not shown). Translation of *cox3-481* mRNA was dependent on wild-type nuclear genes *PET54*, *PET122*, and *PET494*. Taken together, these results demonstrate that sequences at the 5′ end of the *COX3* mRNA are not essential for translational activation.

COX3 is cotranscribed with the upstream tRNA^{Val} gene, and the resulting precursor is subsequently processed between the tRNA and the mRNA (19). Since it was unclear what effect our deletion mutations would have on this processing event, we carried out high-resolution primer extension experiments to map the 5′ ends of the wild-type and mutant *COX3* mRNAs (Fig. 4). Consistent with previous estimates (27, 41), we found that the wild-type *COX3* mRNA 5′-UTL is precisely 613 bases long and begins with the base immediately downstream of the tRNA^{Val}. Interestingly, processing also occurred immediately downstream of the tRNA in both of the short 5′-end deletion mutants tested (*cox3-481* and *cox3-476*) and in a strain carrying a much longer deletion, *cox3-421* (see below) (Fig. 4). Thus, we inferred that the site of precursor cleavage between the tRNA^{Val} and the *COX3* mRNA is determined only by the position of the tRNA.

Deletions, and their revertants, that delimit the target of the translational activators. To localize further the region necessary for translational activation within the upstream half of the *COX3* 5′-UTL, we constructed and phenotypically analyzed a series of increasingly large deletions initiating near the 5′ end of the 5′-UTL: *cox3-512*, *cox3-516*, *cox3-438*, and *cox3-421* (Fig. 1 and Table 2). Deletion of 81 (*cox3-512*) and 125 (*cox3-516*) bases from the 5′ end of the *COX3* 5′-UTL led to reduced

TABLE 2. Detailed descriptions of 5′-UTL mutations

Allele	Description	Plasmid
COX3		pMC241
cox3-4	Δ −605 to +1315	pGW221
cox3-10	Δ −329 to −1	pMC241Δ1
cox3-11	Δ −473 to −1	pMC241Δ2
cox3-12	Δ −593 to −1	pMC241Δ3
cox3-13	Δ −329 to −1; insertion of TATAT between −365 and −364 (revertant of *cox3-10*)	pMC255
cox3-14	Δ −329 to −1; A at −428→T; A at −427→T (revertant of *cox3-10*)	pMC249
cox3-15	Δ −329 to −1 and Δ −437 to −359 (revertant of *cox3-10*)	pMC250
cox3-16	Δ −329 to −1; A at −428→T; A at −423→T (revertant of *cox3-10*)	pMC259
cox3-18	G at −470→A	pMC247
cox3-60	Δ −605 to −344 and −329 to −1	pGW560
cox3-67	Δ −605 to −359 and −329 to −1	pGW567
cox3-160	Δ −585 to −1	pGW160
cox3-421	Δ −605 to −194	pGW421
cox3-429	Δ −605 to −590	pGW429
cox3-438	Δ −605 to −406	pGW438
cox3-446	Δ −605 to −599	pGW446
cox3-476	Δ −608 to −587	pGW476
cox3-481	Δ −613 to −598	pGW481
cox3-512	Δ −607 to −527	pGW512
cox3-516	Δ −605 to −481; A at −479→C	pGW516
cox3-577	Δ −605 to −406; A at −303→T (revertant of *cox3-438*)	pGW577
cox3-590	Δ −605 to −406; A at −311→T (revertant of *cox3-438*)	pGW590
cox3-595	Δ −605 to −406; G at −305→T (revertant of *cox3-438*)	pGW595
cox3-652	Δ −605 to −481 and −329 to −1	pGW652
cox3-662	Δ −605 to −481 and −329 to −1; insertion of TATAT between −365 and −364	pGW662
cox3-666	Δ −605 to −481, −437 to −359 and −329 to −1	pGW666

growth of the respective mutants (GW50 and GW51) on YPEG medium at 30 and 37°C, while both mutants grew like the wild type at 16°C (Fig. 1). Synthesis of the coxIII protein at 30°C was reduced in both mutants compared with that of the wild type (Fig. 3). Both of these deletions also reduced the steady-state levels of *COX3* mRNA at 30°C, to 18% of the wild-type level with *cox3-516* and 13% of the wild-type level with *cox3-512* (Fig. 2). Translation of the mutant mRNAs was dependent on functional copies of *PET54*, *PET122*, and *PET494*. We conclude that while these two deletions affect mRNA stability, they do not remove the target for the translational activators.

Further deletions of 200 (*cox3-438*) and 412 (*cox3-421*) bases in the 5′-UTL prevented respiratory growth (Fig. 1) and blocked coxIII synthesis (Fig. 3). The larger deletion, *cox3-421*, did not affect the mRNA level to a large extent (Fig. 2), while the shorter deletion, *cox3-438*, lowered the mRNA level to 14% of the wild-type level (Fig. 2). This decreased mRNA level alone cannot account for the lack of translation, since it is comparable to that of other respiration-competent mutants. Thus, these two deletions blocked translation.

If a gene codes for a folded three-dimensional macromolecule, one cannot conclude that a deletion which destroys the function directly affects the functionally critical sequences, since indirect effects on the folded structure are likely. For this reason, we attempted to isolate respiring revertants from those deletions that block *COX3* mRNA translation in the hope that secondary changes might restore functionally active structures, giving a more accurate picture of the locations of critical sequences. In a previous study (11), we found that deletions of the downstream 329 bases (*cox3-10*) and the downstream 473 bases (*cox3-11*) both prevented translation (Fig. 1 and Table 2). However, while the larger deletion failed to revert, the smaller one did, suggesting that critical sequences might be located between −329 and −473. All of the 11 respiring revertants isolated from a *cox3-10* mutant strain were found to carry suppressor mutations linked to the mitochondrial genome (see Materials and Methods). Five of these strains, with

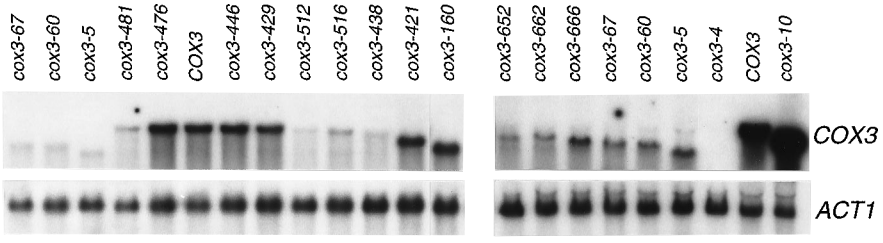

FIG. 2. Steady-state *COX3* mRNA levels in mutants with deletions in the 5′-UTL. RNA was isolated from isogenic strains bearing the indicated *COX3* alleles and analyzed by RNA gel blot hybridization as described in Materials and Methods. The blots were hybridized with a radiolabeled *COX3* probe and subsequently rehybridized with a probe detecting the actin mRNA (*ACT1*). Note that data from two separate experiments are shown; the autoradiogram in the right panel was overexposed to make weak signals more visible. mRNA levels were quantitated by using a Betascope 603 blot analyzer (Betagen Corp.). The relative amounts of *COX3* mRNA were as follows: *COX3* (wild type), 100%; *cox3-10*, 260%; *cox3-160*, 50%; *cox3-481*, 31%; *cox3-476*, 123%; *cox3-446*, 105%; *cox3-429*, 60%; *cox3-512*, 13%; *cox3-516*, 18%; *cox3-438*, 14%; *cox3-421*, 65%; *cox3-652*, 8%; *cox3-662*, 9%; *cox3-666*, 16%; *cox3-67*, 14%; *cox3-60*, 12%; *cox3-5*, 15%.

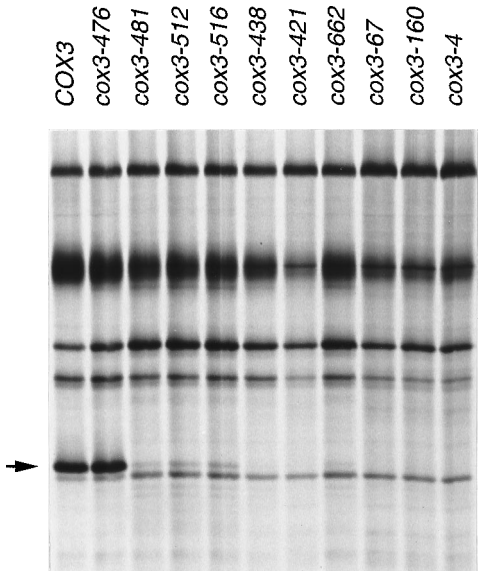

FIG. 3. Mitochondrial translation products in selected *cox3* mutant strains. Mitochondrial translation products were radiolabeled in vivo at 30°C in the presence of cycloheximide and analyzed by sodium dodecyl sulfate gel electrophoresis as previously described (16, 39). The arrow indicates the position of the coxIII protein. The indicated alleles are described in Fig. 1 and Table 2.

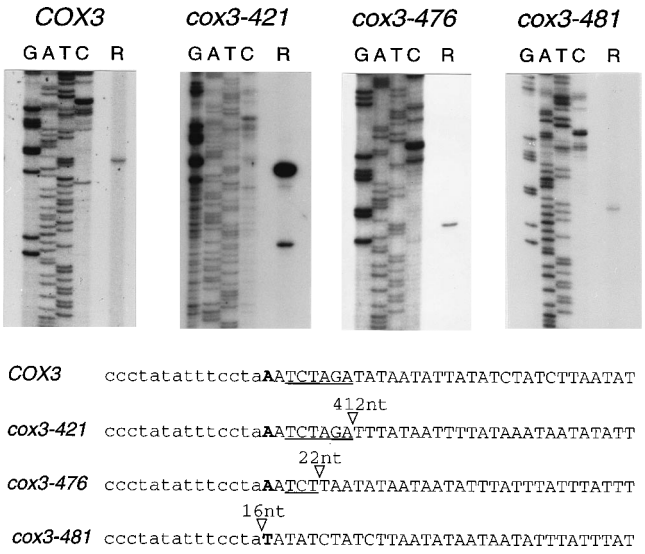

FIG. 4. Primer extension analysis of *COX3* mRNA 5′ ends from the wild type and selected mutants. Primer extension was performed as described in Materials and Methods, by using oligonucleotide oxi2c to prime on RNAs from the wild type (*COX3*), *cox3-476*, and *cox3-481* and oligonucleotide oxi2b to prime on *cox3-421* RNA. (Upper panels) For each indicated allele, primed sequence reactions on cloned template DNAs (GATC) and primed synthesis on RNA templates (R) are shown. (In the overexposed autoradiogram of *cox3-421*, the upper [major] band corresponds to the processing site indicated in the DNA sequence below.) (Lower panel) DNA sequences surrounding the processing sites (complementary to the primer extension products). Lower case letters indicate the $tRNA^{Val}$ coding sequence; uppercase letters indicate the *COX3* mRNA coding sequence. Boldface letters indicate nucleotides corresponding to the 5′ ends of the *COX3* mRNAs. Triangles and numbers above the sequences indicate the positions and sizes (in nucleotides [nt]) of deleted sequences in the mutants. The *Xba*I site near the mRNA 5′ end is underlined.

phenotypes ranging from wild-type to weak respiratory growth (Fig. 5A), were examined further (one of the five has been described previously [11]). All five revertants synthesized the coxIII protein at levels roughly corresponding to their respiratory growth phenotypes (data not shown).

The *COX3* gene was cloned from the *cox3-10* revertant strains, and the nucleotide sequences of their 5′-UTL coding regions were determined. All of the five revertants analyzed carried the parental *cox3-10* deletion of nucleotides −329 to −1 and had additional alterations in the remaining 5′-UTL sequence. Two of the revertant strains, both of which showed wild-type respiratory growth, carried the same nucleotide sequence change, termed *cox3-13*, although they arose independently: a five-base insertion, TATAT, between bases −365 and −364 (Fig. 5A). Another revertant had two adjacent base substitutions: two A residues, at positions −428 and −427, were replaced by two T residues (the *cox3-14* allele) (Fig. 5A). In these two cases, genetic mapping confirmed that the suppressors were linked to *cox3* (Materials and Methods). The fourth revertant, which exhibited a very weak respiratory growth phenotype, had two nonadjacent substitutions: the A residues at positions −428 and −423 were both replaced by T residues (the *cox3-16* allele) (Fig. 5A). The fifth revertant strain, described previously (11), carried an additional 79-base deletion (−437 to −359; the *cox3-15* allele) that conferred cold-sensitive respiratory growth (Fig. 5A). For all five strains, the nucleotide sequence changes described above were the only differences from the wild type in the entire region encoding the 5′-UTL. Importantly, translation of each of these five altered mRNAs was dependent upon activation by nuclear genes *PET54*, *PET122*, and *PET494*, as shown by crosses of the revertants to rho^0 strains bearing null mutations in the nuclear genes.

Similar results were obtained from reversion analysis of the upstream 200-base deletion (*cox3-438*) and the upstream 412-base deletion (*cox3-421*); the larger deletion did not yield mitotically stable revertants (see above), but the smaller one did, suggesting the presence of important sequences between −194 and −406. Genetic analysis of the *cox3-438* revertants (Materials and Methods) revealed that some carried suppressor mutations in mtDNA while others carried nuclear suppressor mutations. Three mitochondrial suppressors, each of which partially restored respiratory growth, were investigated further. DNA encoding the *COX3* 5′-UTL was amplified from each revertant by PCR, and sequence analysis was performed directly on the amplified DNA. In each case, a single-nucleotide change was found in the region between −303 and −311 (Fig. 5B); in the suppressor termed *cox3-590*, T replaced A at −311; in *cox3-595*, T replaced G at −305; and in *cox3-577*, T replaced A at −303. To be sure that these changes were responsible for the suppressor phenotype of the revertants and to exclude the possibility of any additional mutations in the mitochondrial genome, the PCR products carrying the mutated leader versions were cloned, sequenced, and used to transform yeast mitochondria. Integration of the mutated leaders into otherwise wild-type mtDNA restored the original suppressor phenotype in each case. Finally, translation of the three *cox3-438* revertant mRNAs was dependent on nuclear genes *PET54*, *PET122*, and *PET494.*

The *cox3-438* revertants carrying nuclear suppressors were investigated by crossing to three rho^0 strains with null *pet54*, *pet122*, and *pet494* mutations, respectively (MCC90rho^0, TWM21-11Brho^0, and MCC103rho^0; Table 1). Two of the suppressors were unlinked to any of the three genes, but three distinct suppressors were linked to *pet122*: 10 PD:0 NPD:0 T in each case. The missense mutation *PET122-L195* has previously been shown to suppress the cold-sensitive *cox3-15* allele (11),

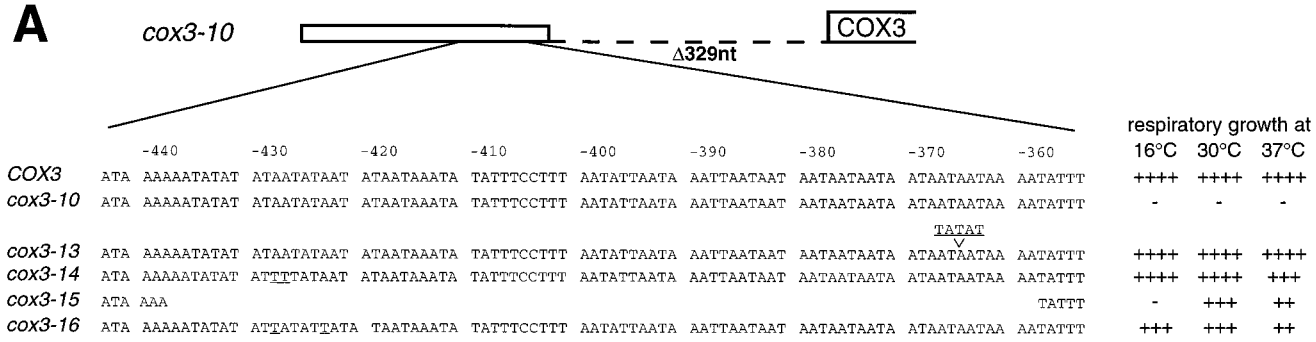

FIG. 5. 5′-UTL sequence alterations and growth phenotypes of mitochondrial revertants of the *cox3-10* and *cox3-438* deletion mutations. (A) The *cox3-10* mutation deleted 5′-UTL bases −329 to −1 (Fig. 1 and Table 2). The wild-type (*COX3*) 5′-UTL coding sequence is shown from bases −440 to −354, the region in which revertants of *cox3-10* had 5′-UTL sequence alterations. Insertions and substitutions in revertants *cox3-13*, *cox3-14*, and *cox3-16* are indicated by the underlined bases. Bases deleted in revertant *cox3-15* are absent. (B) The *cox3-438* mutation deleted 5′-UTL bases −605 to −406 (Fig. 1 and Table 2). The wild-type (*COX3*) 5′-UTL coding sequence is shown from bases −320 to −301, the region in which revertants of *cox3-438* had 5′-UTL sequence alterations. Substitutions in revertants *cox3-590*, *cox3-595*, and *cox3-577* are indicated by the underlined bases. Respiratory growth phenotypes for both sets of revertants were determined as described in the legend to Fig. 1. nt, nucleotides.

but *PET122-L195* did not suppress *cox3-438*. Similarly, the three new apparent *PET122* alleles failed to suppress *cox3-15*; indeed, they appeared to reduce respiratory growth of a *cox3-15* mutant (data not shown). They did improve the respiratory growth of strains carrying the *cox3-512*, *cox3-516*, *cox3-590*, *cox3-595*, *cox3-577* (described above), and *cox3-662* (see below) alleles. However, they failed to suppress the respiration-deficient phenotype caused by *cox3-421* (described above), *cox3-67*, and *cox3-60* (see below).

Taken together, the data in this section strongly suggest that sequences critical for the action of *COX3* mRNA specific activator proteins are located in the region of the 5′-UTL retained in both *cox3-10* and *cox3-438*, bases −405 to −330. To determine whether this region might be sufficient for translation, we crossed haploids bearing these mutations and examined the mtDNA of the recombinant respiring diploid progeny. While we found the wild-type recombinant products among these diploids, we could not find the reciprocal products containing only bases −405 to −330 (data not shown), suggesting that they are not sufficient for respiratory growth.

Construction of a short, partially functional 5′-UTL. To further define the translational activation target in the 5′-UTL, we used information gained from the above-described analysis to guide the construction of shorter versions of the 5′-UTL and tested their function in vivo. First, we combined the upstream 125-base deletion of the partially functional *cox3-516* allele with the downstream 329-base deletion of the nonfunctional *cox3-10* allele and its functional revertants *cox3-13* and *cox3-15*. Thus, by deleting the bases corresponding to −605 to −481 from *cox3-10*, *cox3-13*, and *cox3-15*, we generated the complex mutations *cox3-652*, *cox3-662*, and *cox3-666*, respectively (Fig. 1 and Table 2). Strains carrying all three of these complex alleles accumulated low levels of *COX3* mRNA (approximately 10% of the wild-type level; Fig. 2). The *cox3-652* and *cox3-666* mutants failed to respire at any of the temperatures tested. However, the *cox3-662* mutant strain was able to grow, albeit very weakly, on YPEG medium at 16 and 30°C but not at 37°C and synthesized very small amounts of the coxIII protein at 30°C (Fig. 3). Importantly, the respiratory growth of *cox3-662* mutants was dependent upon functional *PET54*, *PET122*, and *PET494* nuclear genes. Thus, these results confirm that the 151 bases between −481 and −329 contain sequences that can respond to the translational activator proteins when modified by insertion of UAUAU between bases −364 and −365. Presumably, this insertion, selected to restore function to the *cox3-10* deletion, allows the formation of an active structure in the shortened 5′-UTL.

We next attempted to further define the translational activation target by constructing a 5′-UTL, termed *cox3-67*, containing only the 37 bases present in both the partially functional *cox3-15* allele and the *cox3-438* deletion (Fig. 1 and Table 2). While *cox3-438* itself was inactive, it could be activated by single-base changes in the remaining 5′-UTL and by apparent *PET122* mutations (described above). We also con-

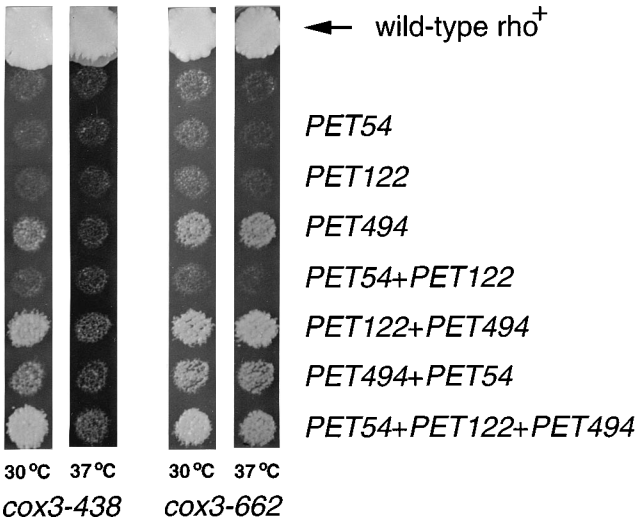

FIG. 6. Overexpression of the translational activators enhances respiratory growth of the *cox3-662* mutant and partially suppresses the *cox3-438* mutation. Strains GW84 (*cox3-438*) and GW146 (*cox3-662*) were transformed with all possible combinations of plasmids causing overproduction of the indicated translational activator proteins (see Materials and Methods). All transformants contained three plasmids, either plasmids directing translational activator overproduction or empty vectors, such that all strains were prototrophic. Transformants were patched on SD plates (see Materials and Methods) and, after incubation at 30°C for 1 day, replica plated to YPEG plates which were incubated at 30 or 37°C as follows: *cox3-662*, 5 days at 30 or 37°C; *cox3-438*, 10 days at 30°C or 13 days at 37°C. Wild-type strain PTY22 (top row) and both mutant strains (second row from the top) were transformed with three empty vectors as controls.

structed an even smaller version, *cox3-60* (Fig. 1 and Table 2). While strains containing both of these mutations accumulated the *COX3* mRNA in amounts comparable to those of other respiring mutants (14% for *cox3-67* and 12% for *cox3-60*; Fig. 2), they failed to grow on YPEG medium, indicating that the mRNAs were not translated, a conclusion confirmed for *cox3-67* (Fig. 3). Neither allele was suppressed by the *PET122*-linked suppressors of *cox3-438*, and neither allele could be reverted. Thus, sequences flanking this apparent core region are necessary for translational activation.

Overproduction of translational activator proteins suppresses the respiratory deficiency of *cox3-438* and improves expression of *cox3-662*. The *COX3* mRNA 5′-UTLs of *cox3-438* and *cox3-662* mutant strains contain translational activation targets that either fail to function under normal conditions or function poorly, respectively. If these targets function poorly because their ability to interact with the genetically defined translational activator proteins is compromised, then overproduction of the proteins might improve the functional interaction and respiratory growth. In the case of the cold-sensitive *cox3-15* allele, overexpression of *PET494* or co-overexpression of *PET494* and *PET122* caused partial suppression (11).

To test the responses of *cox3-438* and *cox3-662* mutants to increased levels of activator proteins, we transformed isogenic strains carrying each mitochondrial mutation with plasmids directing overproduction of all possible combinations of the three proteins (Fig. 6 and Materials and Methods). Suppression at 30 and 37°C was tested by growing patches of the transformants on selective glucose medium for a day and then printing the patches on YPEG plates. At 30°C, respiratory growth of the *cox3-438* mutant was insensitive to overexpression of either *PET54* or *PET122* or overexpression of both *PET54* and *PET122*. However, *cox3-438* was partially suppressed by overexpression of *PET494* at 30°C. This suppression was improved by overexpression of both *PET122* and *PET494* but not by overexpression of both *PET54* and *PET494*. The strongest suppression of *cox3-438* was observed by overproduction of all three proteins together at 30°C. However, *cox3-438* was not suppressed by overproduction of any combination of activators at 37°C.

The *cox3-662* mutant, whose *COX3* mRNA bears a short, partially functional 5′-UTL, exhibited a similar pattern of responses to overexpression of the activator proteins at 30°C (Fig. 6). Essentially the same results were obtained with *cox3-662* at 37°C, except that suppression by overexpression of all three activator genes was weaker at this temperature than suppression by overexpression of *PET122* and *PET494*. In this connection, it is interesting that overexpression of all three activator proteins together actually impairs the respiratory growth of otherwise wild-type strains at 37°C (data not shown).

DISCUSSION

The principal goal of this study was to use deletion mutations to identify sequences within the 613-base *COX3* mRNA 5′-UTL that comprise the target acted upon by the mRNA-specific translational activator proteins PET54, PET122, and PET494. As discussed below, our data suggest that the folded structure of the leader plays an important role in generating the translational activation site. Although the folded structure of this large 5′-UTL is unknown, secondary-structure predictions based on its highly A+U-rich sequence show that it is capable of extensive base pairing (data not shown). The one-dimensional deletion approach to the study of a phenomenon involving a three-dimensional structure is inherently weak. Therefore, we not only examined the phenotype resulting directly from each deletion but also subjected the nonfunctional deletion mutants to a strong selection for suppressor mutations that would restore respiratory growth. In two cases, *cox3-10* and *cox3-438*, this strategy revealed that the untranslatable mutant 5′-UTLs retained sequences that could be converted to functional translational activation sites by secondary mutations in the remaining sequence or, in the case of *cox3-438*, by nuclear mutations linked to *PET122*. The 75-base region of overlap retained in both of these deletions, bases −405 to −330, thus appears to contain core sequences necessary for translation. Importantly, two other deletions that lack this core sequence, *cox3-11* and *cox3-421*, failed to revert.

Of the six intragenic suppressors of *cox3-10* and *cox3-438* analyzed here, five affected positions outside of the 75-base region of overlap (Fig. 5 and Table 2). For example, the *cox3-10* revertant termed *cox3-14* resulted from the conversion of two adjacent A residues (−428 and −427) to two T residues in a region deleted in *cox3-438*. Similarly, the *cox3-438* revertant termed *cox3-590* resulted from the conversion of A to T at −311, a position deleted in *cox3-10*. In addition, a previously described revertant of *cox3-10* was due to a further deletion of 79 bases (−437 to −359) (11), 32 of which are absent in *cox3-438*. Only a single revertant of *cox3-10*, termed *cox3-13*, was due to an alteration solely within the 75-base region of overlap: insertion of TATAT between positions −365 and −364. Taken together, these data are most consistent with the hypothesis that the core 75-base region contains the sequences comprising the translational activation site but that compatible flanking sequences are required to allow proper folding. This folded structure would be required either to form a translational activator binding site or to align that site with the translation initiation codon (or both). Consistent with these ideas, a T inserted in the flanking region between bases −428 and −427 produces no detectable phenotype on its own but en-

hances the defects caused by some other mutations affecting *COX3* translation, especially an initiation codon mutation (12). However, we could not consistently rationalize the effects of mutations flanking the core region by inspection of predicted RNA secondary structures (data not shown). We believe that folding problems also account for our difficulties in constructing active *COX3* mRNAs with deletions on both sides of the core sequence. The shortest active 5′-UTL contained 8 bases from the 5′ end of the wild-type mRNA, 151 internal bases including the core region (from −480 to −330), and a TATAT insertion between positions −365 and −364. This version of the mRNA, *cox3-662*, was only partially functional but was translated in an activator-dependent fashion.

The levels of *cox3-662* mRNA were low, and mutations that increased its steady-state level improved respiratory growth (53). However, respiratory growth rates of the *cox3-662* mutant and the *cox3-438* mutant, whose mRNA level was also low, were not simply limited by mRNA levels, since overproduction of translational activator proteins partially suppressed their phenotypes. By overexpressing each translational activator gene individually in mutant cells, we found that only an increase in PET494 levels caused suppression. By overexpressing all possible pairwise combinations and all three proteins together, we obtained results suggesting that in the presence of excess PET494, PET122 becomes limiting and that when these two proteins are in excess, PET54 becomes limiting. Similar, but less robust, suppression by overproduction of the translational activators has been previously reported (11). These data indicate that if there are unknown components of the activator complex, they are not present in limiting amounts. They also suggest the possibility that the activity of the translational activator complex is regulated by modulation of *PET494* expression, which is known to respond to availability of carbon sources and oxygen roughly in parallel with cytochrome oxidase (32).

In two cases of positive translational control in bacteriophage, the binding of activator proteins to the mRNAs appears to antagonize the formation of mRNA structures that inhibit translation (1, 55). *COX3* mRNA translation does not appear to involve such a double-negative scheme for the following reasons. Elimination of the potentially inhibitory upstream AUG in the 5′-UTL had no detectable effect on translation. Deletion of virtually the entire 5′-UTL (*cox3-12* and *cox3-160*) completely blocked translation, and we could not select suppressors of these deletions. Finally, we carried out extensive selections for mitochondrial mutations that bypass the requirement for *COX3*-specific translational activation but did not obtain a mitotically stable revertant with a simple alteration in the 5′-UTL; all such bypass suppressors were mtDNA rearrangements (deletions), carried in an unstable heteroplasmic state with wild-type mtDNA, that placed new 5′-UTLs on the *COX3* coding sequence (8, 41). While these results are all negative, they are most compatible with the idea that the *COX3* mRNA is simply inert translationally in the absence of activator proteins.

Our data do not elucidate the mechanism by which yeast mitochondrial ribosomes identify initiation codons. Previous work has shown that the AUG sequence itself plays a role in start site selection (15, 40). Additional sequence or structural information is apparently also important for specifying the start codon (15, 40), although a Shine-Dalgarno mechanism does not appear to be involved (10, 37, 43). The data in this report and those from a previous study on the revertants of the deletion mutation *cox3-10* (11) indicate that bases immediately upstream of the initiation codon (−329 to −1) are not required for accurate initiation on the *COX3* mRNA. However, it has recently been suggested that bases immediately upstream of the *COB* mRNA initiation codon are required for accurate start site selection but not for translation per se (37). Deletion of *COB* 5′-UTL bases −32 to −5 and their replacement by an *Eco*RI site eliminated translation of an active cytochrome *b* protein but caused production of a novel polypeptide that migrated slightly faster on sodium dodecyl sulfate gels (37). Thus, the deletion may have shifted initiation to a downstream AUG codon in the cytochrome *b* coding sequence, resulting in a shorter polypeptide. However, the possibility that the observed novel polypeptide was due to aberrant translation of an intron-encoded reading frame in either the *COB* or the *COX1* mRNA was not ruled out, and no data on revertants of this *COB* 5′-UTL mutant were reported.

Our findings on the locations of the 5′ termini of mutant *COX3* mRNAs strongly suggest that the cleavage that generates the mature mRNA is the same event that generates the 3′ end of the $tRNA^{Val}$ immediately upstream of *COX3* in the precursor transcript. The position of this cleavage seems to be determined solely by the position of the $tRNA^{Val}$, since none of the 5′-UTL deletions studied moved the cleavage site relative to the $tRNA^{Val}$. Thus, it seems likely that the 5′ end of *COX3* mRNA is generated by the same endonuclease that generates the 3′ end of mitochondrial tRNAs from precursor transcripts (5). This process appears to be similar to the generation of vertebrate mitochondrial mRNAs by processing at sites corresponding to tRNAs (38, 42).

Interestingly, the mechanism generating the *COX3* mRNA 5′ end appears to differ from that which generates the *COB* mRNA 5′ end, although both precursors contain a tRNA upstream of the 5′-UTL sequences. In the well-studied *COB* case, cleavage at the 3′ end of the $tRNA^{Glu}$ generates the tRNA molecule but the 5′ end of the *COB* mRNA is generated by a second cleavage 144 bases downstream, at −954 relative to the start of translation (36). The position of the second, mRNA-generating, cleavage is determined by a site coded within the *COB* mRNA 5′-UTL. Indeed, a deletion that shifted this site very close the upstream $tRNA^{Glu}$ led to the production of a *COB* mRNA whose 5′ end was within the tRNA sequence (36). Accumulation of the *COB* mRNA, and chimeric mRNAs bearing its 5′-UTL, depends specifically on the function of the *CBP1* nuclear gene (6, 35, 36, 52). No corresponding function is known to be required for accumulation of the *COX3* mRNA. However, our data on *COX3* mRNA levels in deletion mutants indicate that elements at the 5′ end and in the upstream third of the 5′-UTL are required for normal stability.

ACKNOWLEDGMENTS

G.W. was a recipient of an Erwin Schrödinger Fellowship from the Fonds zur Förderung der wissenschaftlichen Forschung (Vienna, Austria). This work was supported by National Institutes of Health Research grant GM29362.

We thank Gerhard Adam and Heather M. Dunstan for critically reading the manuscript.

REFERENCES

1. **Altuvia, S., H. Locker-Giladi, S. Koby, O. Ben-Nun, and A. G. Oppenheim.** 1987. RNase III stimulates the translation of the *c*III gene of bacteriophage λ. Proc. Natl. Acad. Sci. USA **84:**6511–6515.
2. **Ammerer, G.** 1983. Expression of genes in yeast using the *ADC1* promoter. Methods Enzymol. **101:**192–201.
3. **Ausubel, F. M., R. Brent, R. E. Kingston, D. D. Moore, J. G. Seidman, J. A. Smith, and K. Struhl.** 1993. Current protocols in molecular biology. John Wiley and Sons, Inc., Boston.
4. **Brown, N. G., M. C. Costanzo, and T. D. Fox.** 1994. Interactions among three proteins that specifically activate translation of the mitochondrial *COX3* mRNA in *Saccharomyces cerevisiae*. Mol. Cell. Biol. **14:**1045–1053.
5. **Chen, J.-Y., and N. C. Martin.** 1988. Biosynthesis of tRNA in yeast mito-

chondria: an endonuclease is responsible for the 3′-processing of tRNA precursors. J. Biol. Chem. **263:**13677–13682.
6. **Chen, W., and C. L. Dieckmann.** 1994. Cbp1p is required for message stability following 5′-processing of *COB* mRNA. J. Biol. Chem. **269:**16574–16578.
7. **Conde, J., and G. R. Fink.** 1976. A mutant of *S. cerevisiae* defective for nuclear fusion. Proc. Natl. Acad. Sci. USA **73:**3651–3655.
8. **Costanzo, M. C., and T. D. Fox.** 1986. Product of *Saccharomyces cerevisiae* nuclear gene *PET494* activates translation of a specific mitochondrial mRNA. Mol. Cell. Biol. **6:**3694–3703.
9. **Costanzo, M. C., and T. D. Fox.** 1988. Specific translational activation by nuclear gene products occurs in the 5′ untranslated leader of a yeast mitochondrial mRNA. Proc. Natl. Acad. Sci. USA **85:**2677–2681.
10. **Costanzo, M. C., and T. D. Fox.** 1990. Control of mitochondrial gene expression in *Saccharomyces cerevisiae*. Annu. Rev. Genet. **24:**91–113.
11. **Costanzo, M. C., and T. D. Fox.** 1993. Suppression of a defect in the 5′ untranslated leader of the mitochondrial *COX3* mRNA by a mutation affecting an mRNA-specific translational activator protein. Mol. Cell. Biol. **13:**4806–4813.
12. **Costanzo, M. C., and T. D. Fox.** A point mutation in the 5′-untranslated leader that affects translation of the mitochondrial *COX3* mRNA. Curr. Genet., in press.
13. **Costanzo, M. C., E. C. Seaver, and T. D. Fox.** 1989. The *PET54* gene of *Saccharomyces cerevisiae*: characterization of a nuclear gene encoding a mitochondrial translational activator and subcellular localization of its product. Genetics **122:**297–305.
14. **Dieckmann, C. L., and R. R. Staples.** 1994. Regulation of mitochondrial gene expression in *Saccharomyces cerevisiae*. Int. Rev. Cytol. **152:**145–181.
15. **Folley, L. S., and T. D. Fox.** 1991. Site-directed mutagenesis of a *Saccharomyces cerevisiae* mitochondrial translation initiation codon. Genetics **129:**659–668.
16. **Fox, T. D., L. S. Folley, J. J. Mulero, T. W. McMullin, P. E. Thorsness, L. O. Hedin, and M. C. Costanzo.** 1991. Analysis and manipulation of yeast mitochondrial genes. Methods Enzymol. **194:**149–165.
17. **Gallwitz, D., and R. Seidel.** 1980. Molecular cloning of the actin gene from yeast Saccharomyces cerevisiae. Nucleic Acids Res. **8:**1043–1059.
18. **Gottschling, D. E., O. M. Aparicio, B. L. Billington, and V. A. Zakian.** 1990. Position effect at S. cerevisiae telomeres: reversible repression of pol II transcription. Cell **63:**751–762.
19. **Grivell, L. A.** 1989. Nucleo-mitochondrial interactions in yeast mitochondrial biogenesis. Eur. J. Biochem. **182:**477–493.
20. **Haffter, P., and T. D. Fox.** 1992. Suppression of carboxy-terminal truncations of the yeast mitochondrial mRNA-specific translational activator PET122 by mutations in two new genes, *MRP17* and *PET127*. Mol. Gen. Genet. **235:**64–73.
21. **Haffter, P., T. W. McMullin, and T. D. Fox.** 1990. A genetic link between an mRNA-specific translational activator and the translation system in yeast mitochondria. Genetics **125:**495–503.
22. **Haffter, P., T. W. McMullin, and T. D. Fox.** 1991. Functional interactions among two yeast mitochondrial ribosomal proteins and an mRNA-specific translational activator. Genetics **127:**319–326.
23. **Hill, J., P. McGraw, and A. Tzagoloff.** 1985. A mutation in yeast mitochondrial DNA results in a precise excision of the terminal intron of the cytochrome *b* gene. J. Biol. Chem. **260:**3235–3238.
24. **Hinnebusch, A. G., and S. W. Liebman.** 1991. Protein synthesis and translational control in *Saccharomyces cerevisiae*, p. 627–735. *In* J. R. Broach, J. R. Pringle, and E. W. Jones (ed.), The molecular and cellular biology of the yeast *Saccharomyces*: genome dynamics, protein synthesis, and energetics, vol. 1. Cold Spring Harbor Laboratory Press, Cold Spring Harbor, N.Y.
25. **Ito, H., Y. Fukuda, K. Murata, and A. Kimura.** 1983. Transformation of intact yeast cells treated with alkali cations. J. Bacteriol. **153:**163–168.
26. **Jackson, R. J., M. T. Howell, and A. Kaminski.** 1990. The novel mechanism of initiation of picornavirus RNA translation. Trends Biochem. Sci. **15:**477–483.
27. **Kloeckener-Gruissem, B., J. E. McEwen, and R. O. Poyton.** 1988. Identification of a third nuclear protein-coding gene required specifically for post-transcriptional expression of the mitochondrial *COX3* gene in *Saccharomyces cerevisiae*. J. Bacteriol. **170:**1399–1402.
28. **Kozak, M.** 1989. The scanning model for translation: an update. J. Cell Biol. **108:**229–241.
29. **Kunkel, T. A., J. D. Roberts, and R. A. Zakour.** 1987. Rapid and efficient site-specific mutagenesis without phenotypic selection. Methods Enzymol. **154:**367–382.
30. **Macejak, D. G., and P. Sarnow.** 1991. Internal initiation of translation mediated by the 5′ leader of a cellular mRNA. Nature (London) **353:**90–94.
31. **Maniatis, T., E. F. Fritsch, and J. Sambrook.** 1982. Molecular cloning: a laboratory manual. Cold Spring Harbor Laboratory, Cold Spring Harbor, N.Y.
32. **Marykwas, D. L., and T. D. Fox.** 1989. Control of the *Saccharomyces cerevisiae* regulatory gene *PET494*: transcriptional repression by glucose and translational induction by oxygen. Mol. Cell. Biol. **9:**484–491.
33. **McMullin, T. W., and T. D. Fox.** 1993. *COX3* mRNA-specific translational activator proteins are associated with the inner mitochondrial membrane in *Saccharomyces cerevisiae*. J. Biol. Chem. **268:**11737–11741.
34. **McMullin, T. W., P. Haffter, and T. D. Fox.** 1990. A novel small subunit ribosomal protein of yeast mitochondria that interacts functionally with an mRNA-specific translational activator. Mol. Cell. Biol. **10:**4590–4595.
35. **Mittelmeier, T. M., and C. L. Dieckmann.** 1990. CBP1 function is required for stability of hybrid cob-oli1 transcript in yeast mitochondria. Curr. Genet. **18:**421–428.
36. **Mittelmeier, T. M., and C. L. Dieckmann.** 1993. In vivo analysis of sequences necessary for CBP1-dependent accumulation of cytochrome *b* transcripts in yeast mitochondria. Mol. Cell. Biol. **13:**4203–4213.
37. **Mittelmeier, T. M., and C. L. Dieckmann.** 1995. In vivo analysis of sequences required for translation of cytochrome *b* transcripts in yeast mitochondria. Mol. Cell. Biol. **15:**780–789.
38. **Montoya, J., D. Ojala, and G. Attardi.** 1981. Distinctive features of the 5′-terminal sequences of the human mitochondrial mRNAs. Nature (London) **290:**465–470.
39. **Mulero, J. J., and T. D. Fox.** 1993. *PET111* acts in the 5′-leader of the *Saccharomyces cerevisiae* mitochondrial *COX2* mRNA to promote its translation. Genetics **133:**509–516.
40. **Mulero, J. J., and T. D. Fox.** 1994. Reduced but accurate translation from a mutant AUA initiation codon in the mitochondrial *COX2* mRNA of *Saccharomyces cerevisiae*. Mol. Gen. Genet. **242:**383–390.
41. **Müller, P. P., M. K. Reif, S. Zonghou, C. Sengstag, T. L. Mason, and T. D. Fox.** 1984. A nuclear mutation that post-transcriptionally blocks accumulation of a yeast mitochondrial gene product can be suppressed by a mitochondrial gene rearrangement. J. Mol. Biol. **175:**431–452.
42. **Ojala, D., J. Montoya, and G. Attardi.** 1981. tRNA punctuation model of RNA processing in human mitochondria. Nature (London) **290:**470–474.
43. **Pel, H. J., and L. A. Grivell.** 1994. Protein synthesis in mitochondria. Mol. Biol. Rep. **19:**183–194.
44. **Pelletier, J., and N. Sonenberg.** 1988. Internal initiation of translation of eukaryotic mRNA directed by a sequence derived from poliovirus RNA. Nature (London) **334:**320–325.
45. **Pon, L., and G. Schatz.** 1991. Biogenesis of yeast mitochondria, p. 333–406. *In* J. R. Broach, J. R. Pringle, and E. W. Jones (ed.), The molecular and cellular biology of the yeast *Saccharomyces*: genome dynamics, protein synthesis, and energetics, vol. 1. Cold Spring Harbor Laboratory Press, Cold Spring Harbor, N.Y.
46. **Rödel, G., and T. D. Fox.** 1987. The yeast nuclear gene *CBS1* is required for translation of mitochondrial mRNAs bearing the *cob* 5′-untranslated leader. Mol. Gen. Genet. **206:**45–50.
47. **Sanger, F., S. Nicklen, and A. R. Coulson.** 1977. DNA sequencing with chain-terminating inhibitors. Proc. Natl. Acad. Sci. USA **74:**5463–5467.
48. **Sherman, F., G. R. Fink, and J. B. Hicks.** 1986. Methods in yeast genetics. Cold Spring Harbor Laboratory Press, Cold Spring Harbor, N.Y.
49. **Sherman, F., and J. W. Stewart.** 1982. Mutations altering initiation of translation of yeast iso-1-cytochrome *c*; contrasts between the eukaryotic and prokaryotic initiation process, p. 301–333. *In* J. N. Strathern, E. W. Jones, and J. R. Broach (ed.), The molecular biology of the yeast *Saccharomyces*: metabolism and gene expression. Cold Spring Harbor Laboratory Press, Cold Spring Harbor, N.Y.
50. **Shine, J., and L. Dalgarno.** 1974. The 3′-terminal sequence of *Escherichia coli* 16S ribosomal RNA: complementarity to nonsense triplets and ribosome binding sites. Proc. Natl. Acad. Sci. USA **71:**1342–1346.
51. **Sprague, G. F., Jr., R. Jensen, and I. Herskowitz.** 1983. Control of yeast cell type by the mating type locus: positive regulation of the α-specific *STE3* gene by the *MATα1* product. Cell **32:**409–415.
52. **Staples, R. R., and C. L. Dieckmann.** 1993. Generation of temperature-sensitive *cbp1* strains of *Saccharomyces cerevisiae* by PCR mutagenesis and *in vivo* recombination: characteristics of the mutant strains imply that CBP1 is involved in stabilization and processing of cytochrome *b* pre-mRNA. Genetics **135:**981–991.
53. **Wiesenberger, G., and T. D. Fox.** Unpublished data.
54. **Witherell, G. W., and E. Wimmer.** 1994. Encephalomyocarditis virus internal ribosomal entry site RNA-protein interactions. J. Virol. **68:**3183–3192.
55. **Wulczyn, F. G., M. Bölker, and R. Kahmann.** 1989. Translation of the bacteriophage Mu *mom* gene is positively regulated by the phage *com* gene product. Cell **57:**1201–1210.
56. **Yaffe, M. P.** 1991. Analysis of mitochondrial function and assembly. Methods Enzymol. **194:**627–643.